

Polarization-dependent ultrafast carrier dynamics in GaAs with anisotropic response

Ya-Chao Li(李亚超), Chao Ge(葛超), Peng Wang(汪鹏), Shuang Liu(刘爽), Xiao-Ran Ma(麻晓冉), Bing Wang(王冰), Hai-Ying Song(宋海英), and Shi-Bing Liu(刘世炳)

Citation: Chin. Phys. B, 2022, 31 (**6**): 067102. DOI: 10.1088/1674-1056/ac422b
Journal homepage: http://cpb.iphy.ac.cn; http://iopscience.iop.org/cpb

What follows is a list of articles you may be interested in

First-principles calculations of structural and electronic properties of $Tl_xGa_{1-x}As$ alloys

G. Bilgeç Akyüz, A. Y. Tunali, S. E. Gulebaglan, N. B. Yurdasan
Chin. Phys. B, 2016, 25 (**2**): 027101. DOI: 10.1088/1674-1056/25/2/027101

Spatially nonlocal effects on optical absorption properties incoupled quantum wells with an applied electric field

Wang Chao-Yang, Wang Guang-Hui
Chin. Phys. B, 2014, 23 (**12**): 127103. DOI: 10.1088/1674-1056/23/12/127103

A theoretical investigation of the band alignment of type-I direct band gap dilute nitride phosphide alloy of $GaN_xAs_yP_{1-x-y}$/GaP quantum wells on GaP substrates

Ö L Ünsal, B Gönül, M Temiz
Chin. Phys. B, 2014, 23 (**7**): 077104. DOI: 10.1088/1674-1056/23/7/077104

The nonlinear optical properties of a magneto-exciton in a strained $Ga_{0.2}In_{0.8}As$/GaAs quantum dot

N. R. Senthil Kumar, A. John Peter, Chang Kyoo Yoo
Chin. Phys. B, 2013, 22 (**10**): 107106. DOI: 10.1088/1674-1056/22/10/107106

High sensitivity Hall devices with AlSb/InAs quantum well structures

Zhang Yang, Zhang Yu-Wei, Wang Cheng-Yan, Guan Min, Cui Li-Jie, Li Yi-Yang, Wang Bao-Qiang, Zhu Zhan-Ping, Zeng Yi-Ping
Chin. Phys. B, 2013, 22 (**5**): 057106. DOI: 10.1088/1674-1056/22/5/057106

Polarization-dependent ultrafast carrier dynamics in GaAs with anisotropic response

Ya-Chao Li(李亚超)[1,2], Chao Ge(葛超)[1,2], Peng Wang(汪鹏)[1,2], Shuang Liu(刘爽)[1,2], Xiao-Ran Ma(麻晓冉)[1,2], Bing Wang(王冰)[1,2], Hai-Ying Song(宋海英)[1,2,†], and Shi-Bing Liu(刘世炳)[1,2,‡]

[1] *Strong-field and Ultrafast Photonics Laboratory, Key Laboratory of Trans-scale Laser Manufacturing Technology, Ministry of Education, Faculty of Materials and Manufacturing, Beijing University of Technology, Beijing* 100124, *China*

[2] *Strong-field and Ultrafast Photonics Laboratory, Beijing Engineering Research Center of Laser Technology, Faculty of Materials and Manufacturing, Beijing University of Technology, Beijing* 100124, *China*

(Received 4 November 2021; revised manuscript received 7 December 2021; accepted manuscript online 11 December 2021)

The transient dynamics of anisotropic properties of GaAs was systematically studied by polarization-dependent ultrafast time-resolved transient absorption. Our findings revealed that the anisotropy of reflectivity was enhanced in both pump-induced and probe-induced processes, suggesting an extraordinary resonance absorption of photon–phonon coupling (PPC) with intrinsic anisotropic characteristic in carrier relaxation, regardless of the concrete crystallinity and orientation of GaAs sample. The results, delivering in-depth cognition about the polarization-dependent ultrafast carrier dynamics, also proved the paramount importance of interaction between polarized laser and semiconductor.

Keywords: ultrafast pump-probe, polarization-dependence, photon–phonon coupling, GaAs

PACS: 71.36.+c, 78.47.J–, 82.53.–k, 78.47.js **DOI:** 10.1088/1674-1056/ac422b

1. Introduction

The developing and reforming of ultrashort pulse in physical phenomena and real-world applications have attracted more and more research work recently. Microscopic interaction between light and matter was generally studied and discussed.[1–3] It is significantly affected by the polarization of photons when photons interact with quasi-particles such as electrons, phonons, and polariton.[4,5] The polarization of photons is closely related to the anisotropic crystals with periodic structure and long-range order, delivering variable properties responding to the light with different vibration direction.[6,7] The optical anisotropy of carrier transitions and relaxation processes in the crystals is essentially the result of the anisotropy of the interaction between the quasi-particles and the electromagnetic field of incident light. Recently, the development of ultrafast time-resolved technology provides an effective tool for investigating the microscopic interaction of light and matter on critical timescales, which can reflect a lot of significant information for the effect of incident light with different polarization on the matter.[8–10] Therefore, it is meaningful for the manifestation of microscopic optical anisotropy in various ultrafast processes such as interband excitation, thermalization, energy relaxation, and carrier migration, which cannot be realized through traditional anisotropy measurement methods such as Raman spectroscopy[11–13] and x-ray diffraction (XRD),[14–16] etc.

As a prototype of the second generation semiconductor after silicon and germanium, gallium arsenide (GaAs) possesses the higher light absorption coefficient and direct bandgap characteristics.[17–20] These fascinating properties make GaAs highly promising for applications in the field of microelectronics and optoelectronics such as photodetectors,[21,22] infrared light-emitting diodes (LED),[23] laser diodes[24] and solar cells.[25–27] In addition, Smith *et al*. studied the biexcitons of GaAs quantum wells by pump-probe in 1994. It was found the strong influence of the biexciton state on the nonlinear response.[28] Alexandrou *et al*. investigated the evolution of a non-equilibrium photoinjected electron population independent of the hole population in intrinsic GaAs by using the femtosecond pump-probe spectroscopy in 1995.[29] Quochi *et al*. studied Coulomb and carrier dynamics in self-assembled InAs/GaAs quantum dots at room temperature by two-color tunable pump-probe transmission experiments in 2003.[30] Hebling *et al*. observed the recovery of the free-carrier in GaAs by time-resolved THz pump-THz probe measurements in 2010.[31] Nie *et al*. studied transient metal-insulator transition (MIT) of GaAs by ultrafast time-resolved reflectivity and found that the transition temperature was as high as ∼230 K and ∼180 K respectively in 2018.[19] These works fully imply that GaAs play a vital role in the nonlinear optical study of the interaction between ultrashort pulse lasers and semiconductors.

However, the scattered light after the polarized light interacting with the target will contain the polarization infor-

†Corresponding author. E-mail: hysong@bjut.edu.cn
‡Corresponding author. E-mail: sbliu@bjut.edu.cn

© 2022 Chinese Physical Society and IOP Publishing Ltd

mation determined by the target's own characteristics. And the kind of polarization information is different from the spectrum, light intensity, and phase information we usually detect. Based on the polarization information, we can accurately obtain the properties of the measured sample. For example, the surface roughness and internal structure of the tested object can be obtained according to the polarization characteristics of the reflected and transmitted light. Moreover, the easy-to-tune optoelectronic characteristics of GaAs make it a quite appropriate platform for exploring the interaction between light and matter. Despite its unique conditions in optoelectronics, there are few studies on the dynamical anisotropic response of GaAs in the ultrafast processes.

In this paper, we performed ultrafast polarization-resolved pump-probe reflectivity to explore the carrier dynamical response of GaAs under photoexcitation. We confirmed that the polarization modulation of the pump light is of equal importance with probe light for the carrier dynamics process in GaAs. In a constant photoexcited non-equilibrium state, a special oscillation behavior characterized as a "dip" feature during the carrier relaxation process attracts our attention suggesting excited-state absorption (ESA) initial signals in GaAs. Through analysis, the photon–phonon coupling (PPC) based on resonance absorption plays an important role in this carrier dynamic process, exhibiting intrinsic anisotropy under different polarized probe pulse appeared both in single crystals and polycrystalline thin films. Our findings reveal the new mechanism of the microscopic interaction between laser with different polarization and GaAs semiconductor in ultrafast process.

2. Method

Ultrafast polarization-resolved pump-probe transient absorption measurements were performed to elucidate the hot carrier dynamics of n-type bulk single crystal and polycrystalline thin film GaAs using a two-beams pump-probe setup, in which infrared pulses were generated by a mode-locked Ti: sapphire regenerative amplifier system working at 1 kHz repetition rate, centered at 800 nm. Both the pump and probe beam can be deflected by the $1/4\lambda$ wave plate and polarizer to focus on the surface of the materials, with spot sizes at ~ 400 μm (pump) and ~ 200 μm (probe) in diameter. The transient reflected probe signal was collected by a Si-based detector and a lock-in amplifier with a sensitivity on the order of 10^{-6}. The time delay between pump and probe pulses was realized by using a motorized delay line. The samples are mounted vertically on the substrate and placed at ambient temperature. In all cases, we maintained a constant and quasi-saturated pumping fluence to ensure that the samples can be excited stably.

3. Results and discussion

3.1. Pump light polarization modulation in GaAs single crystal

The GaAs single crystal with high quality used in this work is an n-type (100) wafer, with a size of 10 mm× 10 mm ×1 mm. As shown in Fig. 1(a), the GaAs belong to the face-centered cubic zinc-blende crystal structure with a lattice constant of 5.65 Å. The difference in the ability to attract electrons of arsenic and gallium atoms makes the covalent Ga–As bond with certain ionic characteristics, which is between the covalent semiconductor silicon and the ionic semiconductor cadmium sulfide, thus leading to unique properties. Furthermore, GaAs is a typical direct bandgap semiconductor with a band-gap width of 1.424 eV at room temperature. Here, a 800 nm (1.55 eV) laser beam slightly higher than the bandgap of GaAs was employed for the pump light, varying the polarization angle from 0° to 360° in a 45° step. Figure 1(b) shows a schematic diagram of the polarization-dependent pump light acting on the GaAs (100) surface. The reflection system is excited by a pump pulse beam to non-equilibrium state and tracked by a subsequent probe pulse beam. We use the transient reflectivity of probe light to monitor the transient carrier dynamic changes of the system. The differential reflection signal $\Delta R/R_0$ with a specific delay time was collected, defined as

$$\Delta R/R_0 = (R - R_0)/R_0, \tag{1}$$

where R and R_0 are the probe reflectivity of the sample modulated with and without the presence of the pump pulse beam, respectively. It is worth mentioning that the probe light is so weak that the excitation of the sample is negligible, characterizing an intrinsic dynamic change of hot carriers. Thus the interband excitation of the sample is dominated by the pump light.

As demonstrated in Fig. 1(d), we can see the polarization-resolved pump-probe differential reflection signal $\Delta R/R_0$ changes widely with the polarization angle from 0° to 360° in a whole range in carrier relaxation. The absorption to pump photons of GaAs generates a large number of hot free carriers (at T_1 time, see Fig. 1(c)), which includes free electrons in the conduction band (CB) and holes in the valence band (VB) at non-equilibrium state,[32] and making the transient reflectivity rise sharply.[33,34] In fact, the sharp $\Delta R/R_0$ rising edge is an initial signal of the ground state of bleaching (GSB).[35,36] Once the sample in the ground state is injected and excited by the pump photons to the higher excited state, accordingly, the absorption of the probe light is sharply reduced, i.e., the transient reflection signal of probe light received by the detector is significantly higher than the initial value ($\Delta R/R_0 > 0$). Then all the curves with the different polarization angles would reach the maximum value at T_2 time (see Fig. 1(d)), due to the

thermalization process such as electron–electron (e-e) scattering and electron–phonon (e-ph) scattering shown in Fig. 1(c).

It is worth noting that there was an oscillation behavior indicated as the $\Delta R/R_0$ signal between the time T_1 and T_2, of which a new "dip" feature appeared on the characteristic line at 0.7 ps and the signal strength changes periodically with the polarization direction of the pump light, as shown in the illustration in Fig. 1(d). Not only that, the curve signals corresponding to the polarization angles such as 45°, 225°, 90° and 270° even reached negative values. The intensity of the excitation light used in the experiment is constant and the carrier can be regarded as quasi-saturated absorption to the photons, so it is reasonable to speculate that the new "dip" feature is the ESA initial signal in the transient absorption spectra.[35] The main basis for this speculation includes the follows. (i) It appears after the initial signal of GSB and is closely connected, and (ii) the time scale of 700 fs corresponds to the electron–electron interaction, at this time the hot electrons in the excited state can be reabsorbed by the probe light.

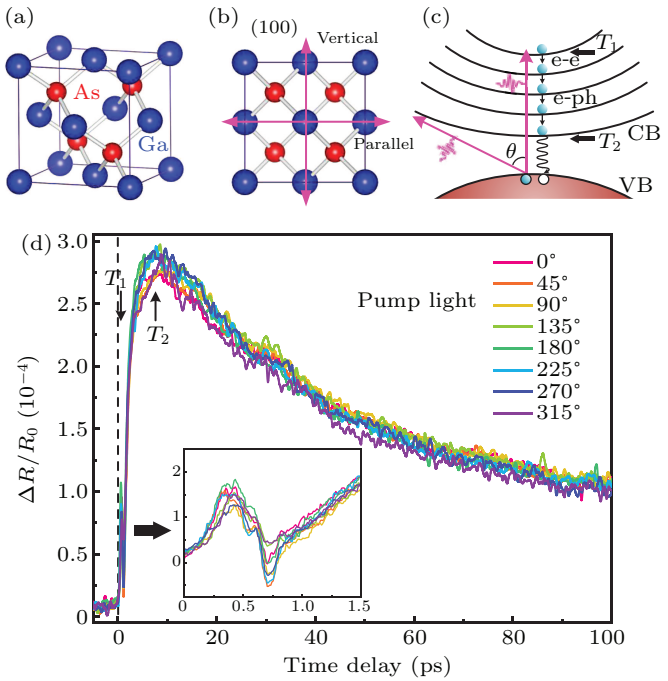


Fig. 1. Polarization-dependent of pump light ultrafast time-resolved transient absorption results. (a) Crystal structure of GaAs. (b) schematic diagram of the polarization-dependent pump light acting on the GaAs(100) surface. (c) Photoexcitation and relaxation processes of pump light at different polarization angle θ. The initial photoexcitation time is denoted as T_1, and the bottom of the low CB (BCB) buildup time is marked as T_2. Hot electrons from the high CB (T_1) lose energy and accumulate to the bottom of the low CB (T_2) via e-e scattering and e-ph scattering. (d) Transient absorption reflectivity changes as a function of pump-probe delay at different pump polarization directions. The zero time delay is determined by the vertical dotted line, which is the cross-correlation of the pump and probe beams, with FWHM of 120 fs. The inset is an enlarged view of the main polarization affected area after precise scanning (see below).

To verify the conjecture, we accurately scanned the oscillation region of the transient reflectivity $\Delta R/R_0$ between the time T_1 and T_2. As shown in Fig. 2(a), the time-scale ranges from -1 ps to 3 ps, and the polarization angle changes from 45° to 135°. Considering the initial stage of the interaction between laser and material ($\Delta R/R_0 > 0$, the differential absorption $\Delta A < 0$), the peak feature in the upper left corner is regarded as the GSB initial signal. The peak differential reflection signals at around 0.4 ps have a special periodic change, which decreases monotonically from 45° to 90°, and then increases from 90° to 135°, exhibiting the GSB initial signals of GaAs single crystal is anisotropic, as shown in Figs. 2(a) and 2(c). Since the peak differential reflection $\Delta R/R_0$ signals are linearly proportional to the differential carrier concentration $\Delta n/n_0$,[37] the polar plots of $\Delta R/R_0$ signals at all polarizations (see Fig. 2(c)) could illustrate the polarization dependence of the injected carrier density. Apparently, the injected carrier density reaches the maximum when the pump polarization direction is along 45°, 135°, 225° and 315°, respectively, indicating the absorption rate at these polarization angles is maximum, i.e., there are relatively more electrons in the VB with the direction of motion at these polarization angles paralleling to the direction of the electromagnetic field of laser, which is dependent on the polarization direction of laser with the corresponding electric vibration vector $\boldsymbol{E}$ of photons. Thus it has an enhanced effect on the transient absorption of photons at a certain polarization direction, resulting in increased height and density of the free electrons in the CB. As shown in Fig. 1(b), the pump light is irradiated vertically on the (100) surface of GaAs. Due to its face-centered cubic structure, the vertical and parallel polarization directions of the excitation light acting on the (100) surface have the same effect. This phenomenon of pumped polarization-dependent GSB initial signals is of important guidance for laser modulation in various GaAs optoelectronic devices.

Then, a "dip" feature appears in the transient reflectivity for the delay time at around 0.7 ps, and inconceivably, it even shows a negative value ($\Delta R/R_0 < 0$) with the polarization direction from 90° to 45°. In addition, the "dip" values gradually decrease with the polarization angle from 135° to 45°, whose periodic change is obviously different from the GSB initial signals. Because it is not simply the excitation behavior of the pump pulse beam and a certain crystal plane. To better reflect the anisotropy of the "dip" values, we have also drawn a polar plot, as shown in Fig. 2(d). The phenomenon of signal reversal after pump light excitation (0.7 ps) suggests that hot carriers have reabsorbed the probe light, i.e., $\Delta A > 0$. The presence of $\Delta A > 0$ in the probe light in the transient absorption spectra will be considered as the ESA or photoinduced absorption (PIA, $\Delta R/R_0 < 0$) initial signal.[35] Moreover, the pump pulse polarization direction is excited along 45° and 225° (vertical) with the maximum absorption strength. It is worth mentioning that the GSB and ESA signals defined in this work are not the entire ultrafast process of GSB and ESA, but refer to the ini-

tial signals at the beginning of these two processes. Although the mechanism of the pump polarization-dependent ESA initial signals still remains not clear, the significance for the analysis of the ESA process cannot be ignored.

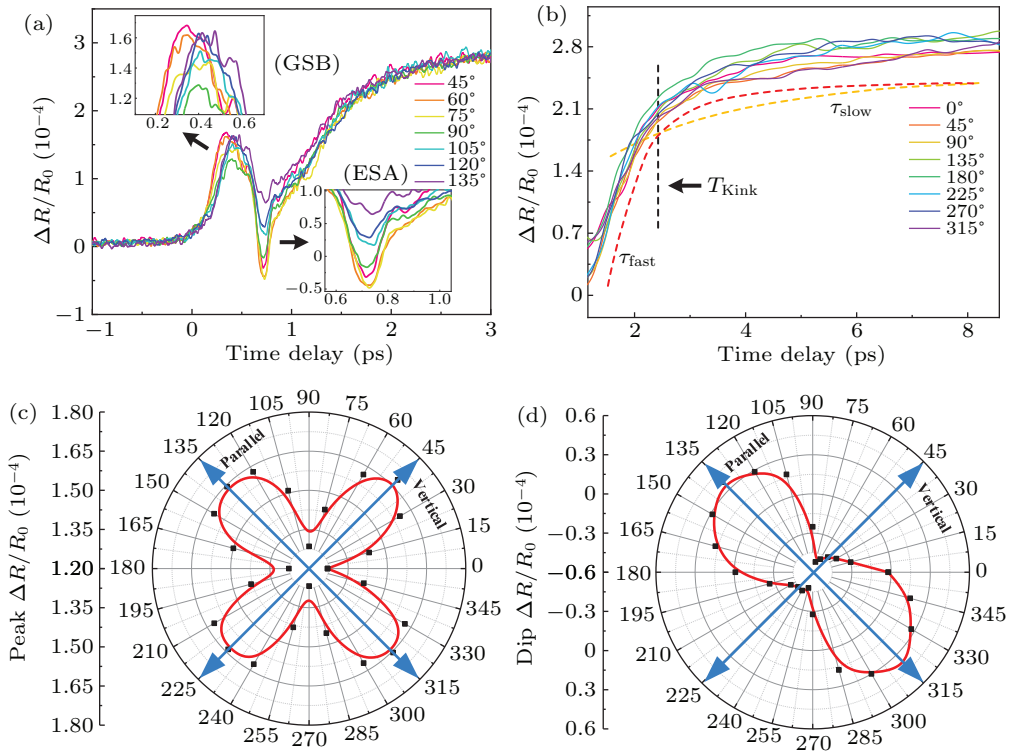


Fig. 2. Polarization-dependent transient absorption results. (a) The time-resolved reflectivity of the polarization dependence of the pump pulse in the oscillating area, with a polarization angle of 45° to 135°. The insets are enlarged views of GSB and ESA initial signals, respectively. Polar plot of peak (c) and dip (d) differential reflection signals of polarization dependence of pump pulse. (b) BCB buildup dynamics between T_1 and T_2. The red and orange dashed lines are single exponential results for decay channels via e-e (fast) scattering and e-ph (slow) scattering. The black dashed line denotes the kink position.

The hot carriers in the higher CB will rapidly return to the bottom of the low CB (BCB) through the thermalization and cooling process after the "dip" feature. A deeper inspection for the dynamic process of the formation BCB is shown in Fig. 2(b), which is zoomed in on the rising edges of Fig. 1(d). As discussed above, the wide rising edges between the time T_1 and T_2 refer to the immediate hot carrier redistribution through the e-e and e-ph scattering channels after the pump beam off. As described in the literature,[38] a universal kink feature in terms of a slope change is clearly observed at a time constant $T_{\text{Kink}} \approx 2.5$ ps, dividing into two time scales: thermalization process τ_{fast} for e-e scattering and cooling process τ_{slow} for e-ph scattering, respectively. We also fit the $\Delta R/R_0$ curves from the time corresponding to "dip" feature to T_2, using a two-component exponential function convolved with a temporal resolution[38]

$$\frac{\Delta R}{R_0}(t) = \left[A_{\max} - A_{\text{fast}} \exp\left(\frac{-t}{\tau_{\text{fast}}}\right) - A_{\text{slow}} \exp\left(\frac{-t}{\tau_{\text{slow}}}\right)\right] R(\delta t), \tag{2}$$

where A_{fast} (τ_{fast}) and A_{slow} (τ_{slow}) represent the amplitude (relaxation time) of fast and slow relaxation, respectively. $A_{\max}$ describes much far slower equilibration processes out of the period of the measurement, such as heat diffusion and Auger recombination. $R(\delta t)$ is a Gaussian curve with FWHM obtained from the cross-correlation measurement. The results show that the thermalization and cooling processes of GaAs are isotropic, of which the relaxation time and intensity are basically unchanged under the different polarized pump pulse excitation ($A_{\text{fast}} \approx 1.1 \times 10^{-3}$, $\tau_{\text{fast}} \approx 0.78$ ps, $A_{\text{slow}} \approx 8.2 \times 10^{-5}$, and $\tau_{\text{slow}} \approx 8$ ps), differing from pump polarization-dependent GSB and ESA initial signals with a prominent anisotropic response.

3.2. Probe light polarization modulation in GaAs single crystal

As mentioned above, we utilize ultrafast time-resolved transient absorption technology to prove that the GSB and ESA initial signals generated by pump light excitation at different polarization direction exhibit anisotropic behavior, of which the cycle time of the GSB initial signals depended on polarization angle is half of the ESA initial signals. To explore the influence of the polarization of the probe light on the hot carrier of the ultrafast process, we modulated the polarization direction of the pump light to 45° (the optimal excitation effect), and then gradually adjusted the polarization direction of the probe light to re-measure. Interestingly, the transient

reflectivity $\Delta R/R_0$ curves in the large-scale pump-probe delay time (-5 ps to 100 ps) are similar to the curves changed by polarization direction of pump pulse as before, as shown in Fig. 3(a). The signal intensity of the "dip" feature in the illustration is also affected by the polarization of the probe light. To research the specific polarization-dependent effect, we accurately scanned the transient reflectivity $\Delta R/R_0$ oscillation region as before. As shown in Fig. 3(b), the values of the "dip" feature signal almost decreases monotonically within the polarization angle changed from 105° to 15°, and negative values also appear at 15° and 30°. Moreover, the transient reflectance signals of the "dip" feature at the whole polarization angle by 15° step are plotted into polar plots in Fig. 3(c), showing obvious polarization dependence of probe pulse.

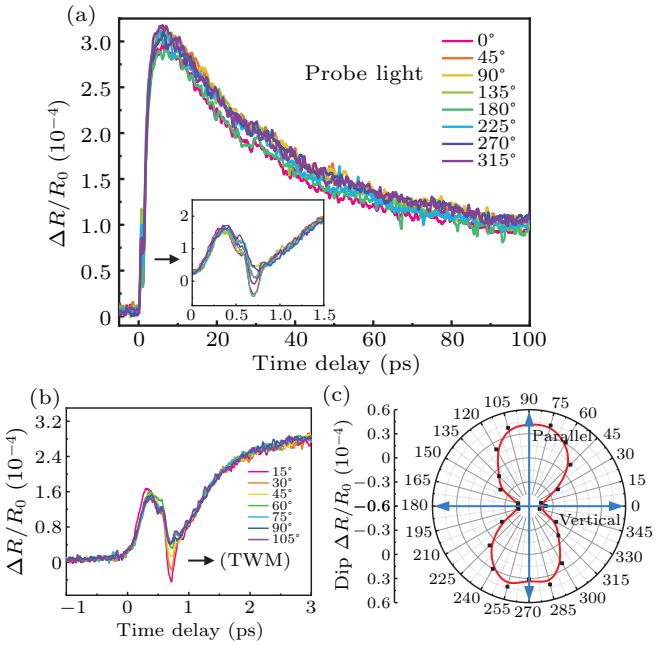


Fig. 3. (a) Polarization-dependent of probe light ultrafast time-resolved transient absorption results. The inset is an enlarged view of the main area of polarization influence. (b) The time-resolved reflectivity of the polarization dependence of the probe pulse in the oscillating area, with a polarization angle of 15° to 105°. (c) Polar plot of dip values of polarization dependence of probe light.

In general, the probe light is used to characterize the dynamic changes of hot carriers, and the effect on the inter-band excitation of the material is usually negligible. Surprisingly, the "dip" feature still appears when only the polarization of the probe light is changed, indicating that GaAs in carrier relaxation do absorb a lot of probe light. The reason lies in two facets: the one is that the free electrons in the excited state will absorb the photon to reach a higher energy excited state under appropriate conditions; the other stronger reason is that the probe light energy may also be resonantly absorbed by polar optical phonons, i.e., PPC as shown in Fig. 4. The coupling behavior occurs when the frequency ω and wave vector $\boldsymbol{k}$ of the photons are exactly the same as the optical phonons by periodic lattice vibrations. Moreover, a directional electric field generated by the lattice vibration will affect the absorption of photons with different electric vibration vector $\boldsymbol{E}$. That is, when the polarization direction of the probe light is consistent with the direction of the electric field, it will enhance the absorption of photons (see Fig. 4), thus the anisotropy of PPC initial signals essentially determines the anisotropy of the ESA initial signals in response to the probe light with the different polarization direction. Furthermore, we call the phenomenon of simultaneous absorption of photons by hot electrons and phonons as three-wave mixing (TWM), as shown in Fig. 3(b). Therefore, the anisotropy of TWM leads to the ESA and the anisotropy responses to the probe light with different polarization.

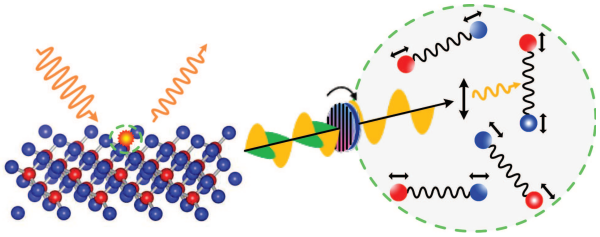


Fig. 4. Schematic diagram of the polarization dependence of the interaction between probe light and optical phonons.

3.3. Probe light polarization modulation in GaAs polycrystal

Considering that the anisotropic behavior of PPC originates from the selective absorption of photons by the directional built-in electric field generated by lattice vibration, phonons play an important role in the anisotropic response of the ESA. Phonons come from the vibration of long-range ordered lattice in crystal, so whether the crystallinity and crystal orientation of crystal will affect the direction of built-in electric field and the anisotropic behavior of PPC deserve further study.

As mentioned above, we selected high quality GaAs single crystals with high orientation and high crystallinity. For comparison, we prepared GaAs thin films with disorderly orientation and poor crystallinity for verification under the same experimental conditions. The thickness of GaAs thin films is 700 nm (> skin depth). The transient reflectivity of GaAs thin films modulated with the polarization angles of the probe pulse from 360° to 180° is shown in Fig. 5(a). Compared with GaAs single crystal, there are several differences in the carrier dynamics of polycrystalline thin films: the residence time of hot carriers on the conduction band is significantly shorter, the exciton lifetime is reduced by nearly an order of magnitude and there is no obvious "dip" feature at the entire measurements. This is mainly due to the fact that the single crystal with strong interatomic binding force and high lattice energy is the most stable state in thermodynamics, thus the hot carriers and excitons in the excited state can stay for a long time. However, the disorder of the atomic arrangement in the polycrystalline thin

films makes GaAs in an unstable state. The hot carriers will quickly reach the bottom of the conduction band through thermal relaxation, and then return to the valence band through interband recombination transition. The disordered arrangement of atoms in the polycrystalline thin films makes the phonon effect significantly enhanced, so the PPC plays an important role in the carrier dynamic process at non-equilibrium state.

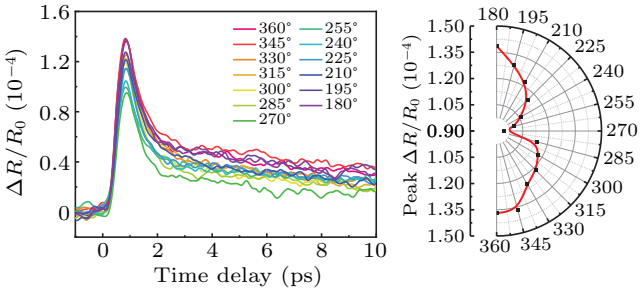


Fig. 5. (a) Polarization-dependent of probe light ultrafast time-resolved transient absorption results of GaAs polycrystalline. (b) Polar plot of peak values of polarization dependence of probe light.

The transient reflectivity still has a certain periodicity when the polarization angle of the probe pulse changes from 360° to 180°, as shown in Fig. 5(a). And the corresponding curves peak intensity change is shown in polar coordinates in Fig. 5(b), of which the periodic variation and curve shape are extremely similar to that of GaAs single crystal in Fig. 3(c). Although the transient reflectivity $\Delta R/R_0$ of GaAs polycrystalline thin films did not show exactly the same curve as before, there is indeed a phenomenon of polarization dependence of the probe beam due to PPC. Consequently, it can be concluded that the anisotropy of PPC based on resonance absorption is an intrinsic property regardless of the crystallinity and orientation of GaAs, even in the polycrystalline thin films that are infinitely close to isotropy.

Then we need to introduce some theoretical models to support our point of view. Simply put the law of conservation of energy and quasi-momentum in a periodic lattice imposes strict restrictions on the coupling between photons and phonons.[4] This is because the wavelength of photons is usually much larger than the distance interatomic. And only phonons with wave vectors in a small area close to the center of the Brillouin zone $k \simeq 0$ can participate in single-phonon scattering. Long-wavelength photons and short-wavelength phonons may still be coupled in the presence of spatial inhomogeneities such as impurities[39] or in disordered materials.[40] Our research object GaAs belongs to a semi-infinite zinc blende polar crystal ($z > 0$). When electromagnetic waves are incident on its (100) surface ($z = 0$) from a vacuum ($z < 0$), the electric field of the incident wave has the following form:[41]

$$\boldsymbol{E}^{\mathrm{i}} = E_0(\cos\phi, \sin\phi, 0)\,\mathrm{e}^{\mathrm{i}q_z z - \mathrm{i}\omega t}, \tag{3}$$

where ω is the frequency and ϕ is the angle between the polarization plane and x-axis which orient along the [100] direction. The electric field of the reflected wave can be expressed as[41]

$$\boldsymbol{E}^{\mathrm{r}} = \left(E_x^{\mathrm{r}}, E_y^{\mathrm{r}}, 0\right)\mathrm{e}^{-\mathrm{i}q_z z - \mathrm{i}\omega t}. \tag{4}$$

In the harmonic approximation, the equations of motions for the atoms can be written as[4]

$$-m_\alpha \omega^2 \boldsymbol{u}_{i\alpha} = e_\alpha \boldsymbol{E}^{\mathrm{T}}\left(\boldsymbol{R}_{i\alpha}\right) + \sum_{j\beta}{}' \boldsymbol{U}_{i\alpha j\beta}\left(\boldsymbol{u}_{j\beta} - \boldsymbol{u}_{i\alpha}\right). \tag{5}$$

Here, m_α and $\boldsymbol{u}_{i\alpha}$ are the mass and the displacement from equilibrium position $\boldsymbol{R}_{i\alpha}$ of the atom α in the ith primitive cell of the crystal. While

$$\boldsymbol{U}_{i\alpha j\beta} = \boldsymbol{K}_{i\alpha j\beta} + e_\alpha \boldsymbol{T}_{i\alpha j\beta} e_\beta / \varepsilon_\infty \tag{6}$$

is the total interaction matrix between atoms $i\alpha$ and $j\beta$. It contains a short-range mechanical term $\boldsymbol{K}_{i\alpha j\beta}$ and a long-range term proportional to the dipolar tensor

$$\boldsymbol{T}_{i\alpha j\beta} = \nabla_{i\alpha}\nabla_{i\alpha}\left|\boldsymbol{R}_{i\alpha} - \boldsymbol{R}_{j\beta}\right|^{-1}. \tag{7}$$

Here, e_α is effective charge, $e_\beta \equiv \pm e^*$, and ε_∞ is the contribution of the valence electrons to the dielectric function.

The first term in Eq. (5) describes the interaction with the retarded transverse field $\boldsymbol{E}^{\mathrm{T}}$ produced by the vibration of the atoms. And this field obeys the wave equation

$$\begin{aligned}&\nabla^2 \boldsymbol{E}^{\mathrm{T}}(\boldsymbol{r}) + \varepsilon_\infty q^2 \boldsymbol{E}^{\mathrm{T}}(\boldsymbol{r}) \\ &= -4\pi q^2 \mathcal{P}^{\mathrm{T}} \sum_{j\beta} e_\beta \boldsymbol{u}_{j\beta}\,\delta\left(\boldsymbol{r} - \boldsymbol{R}_{j\beta}\right),\end{aligned} \tag{8}$$

where $\mathcal{P}^{\mathrm{T}}$ is the transverse projector, $\delta(r)$ is the Dirac delta function and $q = \omega/c$.

Within the bulk of our sample, the equations of motion have Bloch-type solutions[42] $\boldsymbol{u}_{i\alpha} = \boldsymbol{\psi}_{\boldsymbol{k}\alpha}\,\mathrm{e}^{\mathrm{i}\boldsymbol{k}\cdot\boldsymbol{R}_{i\alpha}}$ for which Eq. (5) becomes

$$\begin{aligned}&\sum_\beta \left[\left(m_\alpha \omega^2 - \sum_\gamma \boldsymbol{U}_{\alpha\gamma}(\boldsymbol{0})\right)\delta_{\alpha\beta} + \boldsymbol{U}_{\alpha\beta}(\boldsymbol{k})\right. \\ &\left. + \boldsymbol{U}^{\mathrm{R}}_{\alpha\beta}(\boldsymbol{k})\right]\boldsymbol{\psi}_{\boldsymbol{k}\beta} = 0.\end{aligned} \tag{9}$$

Here

$$\boldsymbol{U}_{\alpha\beta}(\boldsymbol{k}) \equiv \sum_j \boldsymbol{U}_{i\alpha j\beta}\,\mathrm{e}^{-\mathrm{i}\boldsymbol{k}\cdot\left(\boldsymbol{R}_{i\alpha} - \boldsymbol{R}_{j\beta}\right)} \tag{10}$$

is the nonretarded interaction tensor of the Fourier transform, and

$$\boldsymbol{U}^{\mathrm{R}}_{\alpha\beta}(\boldsymbol{k}) = \frac{4\pi q^2 n}{k^2 - q^2\varepsilon_\infty} e_\alpha e_\beta (1 - \hat{\boldsymbol{k}}\hat{\boldsymbol{k}}) \tag{11}$$

is the interaction between sublattices α and β via the radiation field when $q \ll 1/a$, a is the lattice constant and n is the lattice site density. Assuming that the crystal occupies the $z > 0$ region, in this case, Eq. (9) has many solutions: (i) a long-wavelength polariton mode; (ii) some short-wavelength propagating bulk phonons; and (iii) many complex k_z's which correspond to evanescent phonons.[4] For a semi-infinite crystal

with a bulk-truncated, the solution of Eq. (5) can be written as a superposition[43–45] $\boldsymbol{u}_{i\alpha} = \sum_{k_z} \eta_{\boldsymbol{k}} \psi_{\boldsymbol{k}\alpha} \mathrm{e}^{\mathrm{i}\boldsymbol{k}\cdot\boldsymbol{R}_{i\alpha}}$. It completely satisfies the equations of motion for all planes except the N planes closer to the semi-infinite one. Therefore, the infinite system of equations for $\boldsymbol{u}_{i\alpha}$ in Eq. (5) can be simplified to a finite system[4]

$$\sum_{k_z}\left[\sum_{j\beta}^{U}\boldsymbol{U}_{i\alpha j\beta}\left(\psi_{\boldsymbol{k}\alpha}\mathrm{e}^{\mathrm{i}\boldsymbol{k}\cdot\boldsymbol{R}_{i\alpha}}-\psi_{\boldsymbol{k}\beta}\mathrm{e}^{\mathrm{i}\boldsymbol{k}\cdot\boldsymbol{R}_{j\beta}}\right)\right]\eta_{\boldsymbol{k}} = \sum_{j\beta}^{U}\boldsymbol{U}_{i\alpha j\beta}\left(\boldsymbol{u}_{i\alpha}-\boldsymbol{u}_{j\beta}\right)=0. \tag{12}$$

Equation (12) has a direct explanation: the real semi-infinite crystal can be expanded into an artificial infinite crystal by adding imaginary atoms. In addition, in this superposition, the fictitious atoms will not exert any (unretarded) force on the real atoms. The transverse field at the surface[4]

$$\boldsymbol{E}^{\mathrm{T}}(0) = \sum_{k_z\alpha}\eta_{\boldsymbol{k}}\frac{4\pi n q^2}{k^2-q^2\varepsilon_\infty}e_\alpha\mathcal{P}^{\mathrm{T}}\psi_{\boldsymbol{k}\alpha} = \boldsymbol{E}^{\mathrm{i}}+\boldsymbol{E}^{\mathrm{r}} \tag{13}$$

is a superposition of the incident field $\boldsymbol{E}^{\mathrm{i}}$ and all atoms radiated field[4]

$$\boldsymbol{E}^{\mathrm{r}} = \int \mathrm{d}^2 r' \boldsymbol{G}\left(0,\boldsymbol{r}'\right) q^2 e_\alpha \mathcal{P}^{\mathrm{T}} \sum_{i\alpha}\boldsymbol{u}_{i\alpha}\delta\left(\boldsymbol{r}'-\boldsymbol{R}_{i\alpha}\right). \tag{14}$$

Here, $\boldsymbol{G}\left(0,\boldsymbol{r}'\right)$ is the electromagnetic Green's function. In the end, both $\eta_{\boldsymbol{k}}$ and $\boldsymbol{E}^{\mathrm{r}}$ can be calculated and combined with the contribution of the immersed ion to the reflection amplitude $r_i \equiv E^{\mathrm{r}}/E^{\mathrm{i}}$, the reflectivity $R = \left|\left(r_\infty + r_i\right)/\left(1+r_\infty r_i\right)\right|^2$ is obtained from the valence electron polarization contribution r_∞. It can be seen that the electron polarization caused by atomic vibration will affect the resonant absorption of photons (anisotropic transient reflectivity) regardless of single crystal or polycrystalline. Therefore, the coupling between optical phonons and photons is anisotropic. Obviously, this is also a necessary condition to be able to detect polarization-dependent Raman signals.[11]

4. Conclusion

In summary, we studied the anisotropy of hot carrier dynamics in GaAs by polarization-dependent ultrafast time-resolved transient absorption in the presence of photoexcitation. The results provided clear evidence that the initial signal of ground-state bleaching and excited-state absorption are all polarization-dependent with anisotropic response to pump pulse. Further analysis of the crystallinity and orientation of GaAs suggested that resonance absorption of photon–phonon coupling leads to a probe polarization-dependent absorption in carrier relaxation whether in anisotropic single crystals with high crystallinity or in isotropic polycrystalline thin films with the disordered arrangement. The selective absorption of photons by the directional built-in electric field generated by periodic lattice vibration makes photon–phonon coupling and the three-wave mixing with substantial anisotropic behavior. This work reveals insights into the unique carrier dynamics with anisotropic response in GaAs semiconductor, on the other hand, also provides attractive potential application of building high-field and angle-sensitive optoelectronic devices.

Acknowledgement

Project supported by the National Natural Science Foundation of China (Grant Nos. 51875006 and 51705009).

References

[1] Shu C C, Dong D, Petersen I R and Henriksen N E 2017 *Phys. Rev. A* **95** 033809
[2] Bergner K, Flamm D, Jenne M, Kumkar M, Tünnermann A and Nolte S 2018 *Opt. Express* **26** 2873
[3] Shugaev M V, Wu C, Armbruster O, Naghilou A, Brouwer N, Ivanov D S, Derrien T J Y, Bulgakova N M, Kautek W, Rethfeld B and Zhigilei L V 2016 *MRS Bull.* **41** 960
[4] Mochán W L and Récamier J 1989 *Phys. Rev. Lett.* **63** 2100
[5] Knapen S, Lin T, Pyle M and Zurek K M 2018 *Phys. Lett. B* **785** 386
[6] Zhang C, Ouyang H, Miao R, Sui Y, Hao H, Tang Y, You J, Zheng X, Xu Z, Cheng X and Jiang T 2019 *Adv. Opt. Mater.* **7** 1900631
[7] Miao R, Hu Y, Ouyang H, Tang Y, Zhang C, You J, Zheng X, Xu Z, Cheng X and Jiang T 2019 *Nanoscale* **11** 14598
[8] López-Flores V, Arabski J, Stamm C, HaltéV, Pontius N, Beaurepaire E and Boeglin C 2012 *Phys. Rev. B* **86** 014424
[9] Brixner T, García de Abajo F J, Schneider J and Pfeiffer W 2005 *Phys. Rev. Lett.* **95** 093901
[10] Mankowsky R, von Hoegen A, F?rst M and Cavalleri A 2017 *Phys. Rev. Lett.* **118** 197601
[11] Tian N, Yang Y, Liu D, Liu X, Tan P H, Zhang D, Chang K, Li H, Zhao M, Li J R, Tang X, Zhang D, Zhang Z, Xiao W, Yan H and Zhang Y 2018 *ACS Nano* **12** 1712
[12] Liu Y, Gu Q, Peng Y, Qi S, Zhang N, Zhang Y, Ma X, Zhu R, Tong L, Feng J, Liu Z and Chen J H 2018 *Adv. Mater.* **30** 1706402
[13] Song Q, Pan X, Wang H, Zhang K, Tan Q, Li P, Wan Y, Wang Y, Xu X, Lin M, Wan X, Song F and Dai L 2016 *Sci. Rep.* **6** 29254
[14] Kato K, Ito K and Hoshino T 2020 *J. Phys. Chem. Lett.* **11** 6201
[15] Niu S, Joe G, Zhao H, Zhou Y, Orvis T, Huyan H, Salman J, Mahalingam K, Urwin B, Wu J, Liu Y, Tiwald T E, Cronin S B, Howe B M, Mecklenburg M, Haiges R, Singh D J, Wang H, Kats M A and Ravichandran J 2018 *Nat. Photonics* **12** 392
[16] Tung I C, Krishnamoorthy A, Sadasivam S, Zhou H, Zhang Q, Seyler K L, Clark G, Mannebach E M, Nyby C, Ernst F, Zhu D, Glownia J M, Kozina M E, Song S, Nelson S, Kumazoe H, Shimojo F, Kalia R K, Vashishta P, Darancet P, Heinz T F, Nakano A, Xu X, Lindenberg A M and Wen H 2019 *Nat. Photonics* **13** 425
[17] Han Z J, Liu H, Li Q, Zhou D and Lv J 2021 *Chin. Phys. Lett.* **38** 046201
[18] Huang D M, Zhang J Y, Wang J H, Wei W Q, Wang Z H, Wang T and Zhang J J 2021 *Chin. Phys. Lett.* **38** 068101
[19] Nie X C, Song H Y, Zhang X, Gu P, Liu S B, Li F, Meng J Q, Duan Y X and Liu H Y 2018 *New J. Phys.* **20** 033015
[20] You Y Y, Jiang T R and Lai T S 2020 *Chin. Phys. Lett.* **37** 087803
[21] Alzeidan A, Claro M S and Quivy A A 2019 *J. Appl. Phys.* **126** 224506
[22] Geum D M, Kim S, Kim S K, Kang S, Kyhm J, Song J, Choi W J and Yoon E 2019 *Sci. Rep.* **9** 18661
[23] Aziz M, Xie C, Pusino V, Khalid A, Steer M, Thayne I G and Cumming D R S 2017 *Appl. Phys. Lett.* **111** 102102
[24] Mahajan S S, Sharma A, Jain D, Saini H, Yadav B, Naik A A and Jain A 2018 *Vacuum* **152** 128
[25] Chen H, Lee S M, Montenegro A, Kang D, Gai B, Lim H, Dutta C, He W, Lee M L, Benderskii A and Yoon J 2018 *ACS Photonics* **5** 4289
[26] Zhao B, Tang X S, Huo W X, Jiang Y, Ma Z G, Wang L, Wang W X, Chen H and Jia H Q 2018 *Solar Energy* **174** 703

[27] Vaisman M, Jain N, Li Q, Lau K M, Makoutz E, Saenz T, McMahon W E, Tamboli A C and Warren E L 2018 *IEEE J. Photovolt.* **8** 1635

[28] Smith G O, Mayer E J, Kuhl J and Ploog K 1994 *Solid State Commun.* **92** 325

[29] Alexandrou A, Berger V and Hulin D 1995 *Phys. Rev. B* **52** 4654

[30] Quochi F, Dinu M, Pfeiffer L N, West K W, Kerbage C, Windeler R S and Eggleton B J 2003 *Phys. Rev. B* **67** 235323

[31] Hebling J, Hoffmann M C, Hwang H Y, Yeh K L and Nelson K A 2010 *Phys. Rev. B* **81** 035201

[32] Othonos A 1998 *J. Appl. Phys.* **83** 1789

[33] Shank C V, Auston D H, Ippen E P and Teschke O 1978 *Solid State Commun.* **26** 567

[34] Auston D H, McAfee S, Shank C V, Ippen E P and Teschke O 1978 *Solid State Electron.* **21** 147

[35] Guo Z, Wan Y, Yang M, Snaider J, Zhu K and Huang L 2017 *Science* **356** 59

[36] Wei K, Zheng X, Cheng X, Shen C and Jiang T 2016 *Adv. Opt. Mater.* **4** 1993

[37] Ruzicka B A, Wang R, Lohrman J, Ren S and Zhao H 2012 *Phys. Rev. B* **86** 205417

[38] Zhang X, Song H Y, Nie X C, Liu S B, Wang Y, Jiang C Y, Zhao S Z, Chen G, Meng J Q, Duan Y X and Liu H Y 2019 *Phys. Rev. B* **99** 125141

[39] Colwell P J and Klein M V 1970 *Solid State Commun.* **8** 2095

[40] Brodsky M H 1983 *Light Scattering in Solids I* (Berlin, Heidelberg: Springer), pp. 205–251

[41] Pérez-Rodrıguez F, Récamier J and Mochán W L 1998 *Surface Science* **414** 93

[42] Ziman J M 1972 *Principles of the Theory of Solids* (Cambridge: Cambridge University Press)

[43] Mahan G and Obermair G 1969 *Phys. Rev.* **183** 834

[44] Dub P 1981 *Phys. Status Solidi (b)* **104** 109

[45] Mochán W L and Barrera R G 1984 *J. Phys. Colloques* **45** C5–207